

# Delta Wing Vortex Manipulation Using Pulsed and Steady Blowing During Ramp-Pitching

H. Johari\* and J. Moreira†

Worcester Polytechnic Institute, Worcester, Massachusetts 01609

The effectiveness of steady and pulsed blowing as a method of controlling delta wing vortices during ramp-pitching has been investigated in flow visualization experiments conducted in a water tunnel. The recessed angled spanwise blowing technique was utilized for vortex manipulation. This technique was implemented on a beveled 60-deg delta wing using a pair of blowing ports located beneath the vortex core at 40% chord. The injected flow was primarily in the spanwise direction with a component normal to the wing surface. The location of vortex burst was measured as a function of blowing intensity and pulsing frequency in static conditions and the optimum blowing case was applied to the pitching wing. Pulsed blowing, when the natural burst location was upstream of the blowing port, delayed vortex breakdown in static and dynamic cases. Dynamic tests verified the existence of a hysteresis effect and demonstrated the advantages in the control of vortex breakdown offered by pulsed blowing over both steady blowing and no-blowing scenarios. Vortex breakdown responded quasisteadily when the pitchup effects were relatively smaller than the blowing effects. At higher pitching rates, the burst location was affected primarily by the pitching parameters. The application of blowing resulted in expedited vortex reformation during the pitchdown.

## Nomenclature

- $C_\mu$  = blowing coefficient,  $\dot{m}_j V_j / qS$   
 $c$  = root chord length  
 $F$  = reduced blowing frequency,  $2\pi fc / U_\infty$   
 $f$  = blowing frequency, Hz  
 $\dot{m}_j$  = blowing fluid mass flow rate  
 $q$  = freestream dynamic pressure  
 $Re$  = Reynolds number,  $U_\infty c / \nu$   
 $S$  = wing planform area  
 $U_\infty$  = freestream velocity  
 $V_j$  = mean blowing fluid velocity  
 $X_b$  = burst location in presence of blowing  
 $X_n$  = natural (without blowing) burst location  
 $\alpha$  = angle of attack  
 $\dot{\alpha}$  = pitching rate, rad/s  
 $\alpha^*$  = normalized pitching rate,  $\dot{\alpha} c / U_\infty$   
 $\Delta X$  = net change in burst location,  $X_b - X_n$   
 $\nu$  = viscosity

## Introduction

THE flow pattern about delta wings is distinguished by two primary vortices that provide a large portion of lift at high angles of attack. A delta wing's triangular planform causes freestream flow to separate at the leading edges and the separated shear layers form the primary vortices. Through delicate flow visualization, Gad-el-Hak and Blackwelder<sup>1</sup> showed that the leading-edge shear layers consist of a series of discrete vortices analogous to conventional planar shear layers.<sup>2,3</sup> These smaller discrete vortices combine to create the primary vortices. Discrete vortices were found to form at a specific frequency that is dependent on the freestream velocity as well as the angle of attack.<sup>1</sup> Although Gad-el-Hak and Blackwelder<sup>1</sup>

and Lowson<sup>4</sup> both reported a single shedding frequency along the leading edges, recent numerical simulations of Gordnier and Visbal<sup>5</sup> revealed that the shedding frequency of discrete vortices may also be a function of chord location. In any case, the primary vortices are formed from the smaller discrete vortices that have been manipulated by weak perturbations at subharmonic frequencies in planar free shear layers.<sup>6</sup> It was therefore postulated that the shedding frequency could be coupled with a perturbation to alter the primary vortex characteristics.

At high angles of attack, the primary vortices tend to break down or burst; this phenomenon is characterized by the abrupt expansion of the core and the rapid deceleration of the axial velocity. Vortex breakdown reduces the lift created by the primary vortices and the lift coefficient is strongly correlated with the chordwise location of breakdown. To control vortex breakdown on delta wings a number of steady blowing techniques have been explored in the past. Relatively few investigations of unsteady blowing have been pursued. Inspired by the presence of discrete vortices in the free shear layers of delta wings, Gad-el-Hak and Blackwelder<sup>7</sup> experimented with pulsatile injection from slots along the entire leading edges of a stationary delta wing and found that the evolution of discrete vortices could be altered significantly when the forcing frequency was a subharmonic of the natural shedding frequency. The injection velocity was equal to the freestream velocity and the flow was modulated by a solenoid valve driven via a square-wave generator. Vortex breakdown location as a function of frequency and amplitude of perturbation has been recorded by Shi et al.<sup>8</sup> and Gu et al.<sup>9</sup> on stationary delta wings and by Vakili et al.<sup>10</sup> in circular tubes. Meyer and Seginer<sup>11</sup> investigated the effects of periodic spanwise blowing on the lift and drag of a fighter model with a 60-deg sweep angle. At low frequencies the vortex response generally lags behind the forcing by one convective time scale.

With the recent emphasis on the enhancement of fighter aircraft maneuverability, especially during transient motions, behavior of delta wing vortices under various dynamic conditions has been investigated. Both sinusoidal<sup>12–14</sup> and ramp-pitching<sup>15–18</sup> motions have resulted in hysteretic location of the primary vortex breakdown and a nearly constant speed for the motion of burst location. The governing parameter for wings undergoing dynamic conditions is the reduced frequency (si-

Received June 17, 1995; revision received Sept. 8, 1995; accepted for publication Sept. 13, 1995. Copyright © 1995 by H. Johari and J. Moreira. Published by the American Institute of Aeronautics and Astronautics, Inc., with permission.

\*Assistant Professor, Mechanical Engineering Department. Senior Member AIAA.

†Graduate Student, Mechanical Engineering Department. Student Member AIAA.

nusoidal) or the normalized pitching rate (ramp-pitching). Although blowing techniques have been utilized extensively to alter the vortex breakdown location on stationary wings, these techniques have not been attempted on delta wings experiencing transient pitching motions, except in the study of Miller and Gile.<sup>19</sup> This study will be considered in the Discussion section.

In the present effort, the effectiveness of steady and pulsed blowing as a method of delaying vortex breakdown on pitching delta wings has been investigated. The blowing configuration employed was the recessed angled spanwise blowing of Fitzpatrick et al.<sup>20</sup> and is further explained in the next section. A 60-deg delta wing was pitched up at a constant rate from stationary conditions at 18-deg angle of attack to 32 deg and was then pitched down to create a saw-tooth pitching function. Only the first cycle of saw-tooth was studied since this case might reasonably represent the pitching of a delta wing in practice, i.e., rapid pitchup at constant rate followed by pitchdown. Vortex breakdown location was measured by means of flow visualization as a function of pitching rate, blowing coefficient, and pulsing frequency.

### Apparatus

The experiments were conducted in a free-surface water tunnel with a  $60 \times 60$  cm test section at a freestream velocity of 33.5 cm/s. The test stand apparatus consisted of a delta wing, a pitching mechanism, and a blowing fluid delivery system. A 60-deg delta wing with a 25-deg leading-edge bevel, previously used by Fitzpatrick et al.,<sup>20</sup> was modified for the present experiments and is depicted in Fig. 1. The bevel angle was originally chosen to match the detailed study of O'Neil et al.<sup>21</sup> The wing's sharp leading-edge bevel served to fix the separation point of the boundary layers. The wing had a 25.7 cm root chord length, 30 cm trailing-edge span, and 1.9 cm thickness, which resulted in a thickness-to-chord ratio of 7.4%. In absence of blowing, the wing created vortices that burst between the trailing edge and vertex within the  $\alpha$  range of 14–34 deg. For this range of  $\alpha$  the solid blockage ratio varied between 2.6–6%. The Reynolds number based on root chord length and freestream velocity of the tunnel was  $8.6 \times 10^4$ .

Recessed angled spanwise blowing (RASB), which was first studied by Fitzpatrick et al.,<sup>20</sup> uses ports on the delta wing planform to inject fluid in the spanwise direction at an angle parallel to the leading edge bevel, as shown in Fig. 2. A pair of 0.3-cm-diam ports were situated beneath the vortex axis at the 40% root chord line of the wing used in this study, for this position resulted in the maximum effectiveness in delaying breakdown among blowing ports located at 0.20, 0.30, and 0.40c during previous testing.<sup>22</sup> Blowing at angles of attack at which the port was upstream of the natural burst point caused premature bursting of the vortex, while blowing from ports downstream of the natural burst point delayed the onset of vortex breakdown. It has been shown that the burst point at any given angle of attack is oscillatory in nature and RASB appeared to reduce the frequency of this oscillation.<sup>20,22</sup>

The fluid delivery system was designed to provide both steady and pulsed flow for blowing. The customary definition of blowing coefficient  $C_\mu$  ( $=\dot{m}_j V_j / \rho S$ ) was used to nondimensionalize the blowing momentum flux from a single port. According to earlier RASB studies,<sup>20,22</sup> any single port  $C_\mu$  value greater than 0.03 would yield little further effectiveness in delaying vortex breakdown. It is noteworthy that the blowing coefficient in Refs. 20 and 22 was defined for a pair of blowing ports. Since all tubing necessary for both blowing fluid and dye was housed internally in the wing, the thickness-to-chord ratio (7.4%) was therefore uncharacteristically high for a delta wing model and this may have imparted pseudoconical flow characteristics near the apex that could potentially alter the flow details there.<sup>22</sup>

To control the blowing fluid flow, a  $\frac{1}{4}$ -in. needle valve was used for adjusting the flow rate, and a  $\frac{1}{4}$ -in. two-way normally

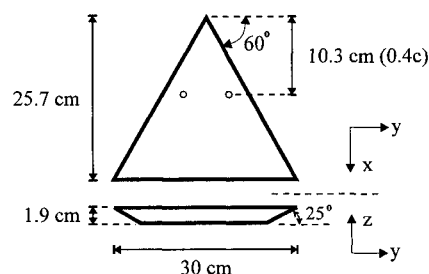


Fig. 1 Delta wing dimensions and blowing ports.

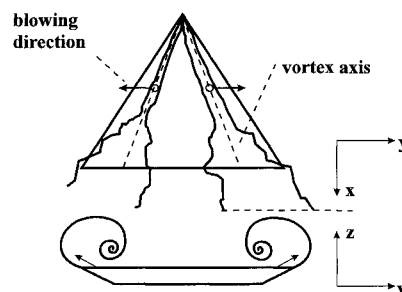


Fig. 2 Schematic of RASB.

open solenoid valve enabled the system to create pulsatile flow. The fluid delivery system was capable of delivering enough fluid to achieve a  $C_\mu$  of 0.1 given the wing geometry and test conditions. A square wave function generator was used for pulsing, the frequency of which was normalized by the root chord length and the freestream velocity following Ref. 11. The reduced blowing frequency  $F$  was therefore equal to  $2\pi f c / U_\infty$ , where  $f$  was the frequency (Hz) supplied by the wave generator. In the present setup, reduced blowing frequencies could be varied in the range of 4.8–72.1, corresponding to 1–15 Hz. A duty cycle of 0.5 was chosen so that the valve would be open for the first half of the cycle and closed for the last half. Systematic variations of duty cycle were not investigated in the present study. Although a square-wave generator was used to control the solenoid valve, the blowing output flow was expected to be a smooth pulse (in time) due to the viscous interactions present in the tubing from the valve exit to the blowing port.

The fluid delivery system was run at a variety of settings and the volume of blowing fluid delivered over a given time period was measured to determine the mean flow rate and blowing coefficient during pulsed operation. Therefore, these measurements were time averages. For pulsed blowing, all  $C_\mu$  values are averages over the pulsing portion when the valve is open, i.e., the time averaged blowing coefficient would be half as much as the steady blowing coefficient. The uncertainty in mean blowing coefficient is estimated to be  $\pm 0.005$ , primarily because of flow meter and volume readings in steady and pulsed cases.

The pitching mechanism, depicted in Fig. 3, consisted primarily of a six-bar linkage that rotated the wing about its quarter-chord line and was based loosely upon a similar one used by Miao et al.<sup>17</sup> Pitching rate  $\dot{\alpha}$  was normalized by the freestream velocity and the root chord length. The pitching mechanism, whose other major components included the linkage's support frame, its motor, the motor control board, a gearbox, and a driving program, was designed to have minimal effect on the flowfield about the wing and to maintain tight tolerances necessary for accurate wing alignment. To avoid linkage-induced flow disruptions, all vertical bars were chamfered and placed at a distance of more than 30 cm aft of the delta wing's trailing edge.

An ac stepping motor was used to drive the mechanism because of the ease with which it changed pitching rates and

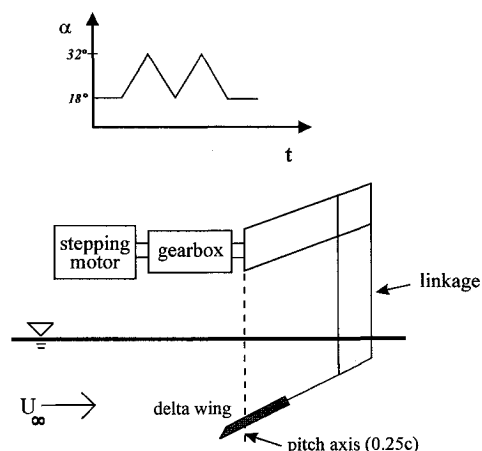


Fig. 3 Pitching mechanism schematic and nominal pitching function ( $\alpha$  vs time).

because of its nearly instantaneous start and stop control capabilities. A computer program was written and installed on a personal computer to control the board that ran the motor and therefore determined the pitching rate. The nominal pitching function ( $\alpha$  vs time) is also shown in Fig. 3. The pitching rate  $\dot{\alpha}$  values were accurate to within  $3.5 \times 10^{-3}$  rad/s (i.e., 0.0025 for the normalized pitch rate  $\alpha^*$ ) based upon the performance of the entire pitching mechanism. The uncertainty in angle-of-attack measurements was on the order of  $\pm 0.5$  deg.

Vortex burst locations were obtained through flow visualization. Black dye was injected into the freestream near the wing vertex and all tests were recorded with a video camera. The wing was placed in the water tunnel with its leeward side facing the transparent floor of the test section to avoid any complications because of the tunnel's free surface, as indicated in Fig. 3. The planform image was captured by reflecting it towards the camera with a mirror placed on an angle-adjustable stand that minimized parallax corrections.

Vortex burst data were obtained visually by playing the video recordings frame-by-frame. For the static runs, the burst location was averaged visually while for the dynamic runs, measurements are single samples. The oscillation magnitude of the vortex burst in static runs was estimated at  $\pm 2.5\%$  of chord length and the average position was used for all analysis. Error margin in reading burst location was concurrently estimated at  $\pm 2.5\%$  of chord length.

## Results

The test series conducted were separated into two phases: 1) static and 2) ramp-pitching. Each phase included no-blowing, steady blowing, and pulsed blowing runs. The static runs were conducted to collect data on the effects of pulsed blowing as well as to compare the present data with the earlier measurements of steady blowing.<sup>22</sup>

### Static Testing

Initially, a series of baseline runs were performed to verify the experimental methods utilized presently. The mean vortex breakdown location was measured with and without blowing for  $\alpha \geq 14$  deg since a well-defined vortex breakdown was not present below this angle of attack. The static test results without blowing are presented in Fig. 4. The present vortex burst location data are compared with that of Fitzpatrick et al.<sup>20</sup> and O'Neil et al.<sup>21</sup> Except for  $\alpha = 14$  and 22 deg, the present data agree with the wind-tunnel measurements of O'Neil et al.<sup>21</sup> to within experimental uncertainty. The data of Fitzpatrick et al.<sup>20</sup> are also close to the present data until 22 deg, beyond which the present data are nearly identical with the other study. The vortex burst was located above the blowing port at an angle of attack of approximately 19 deg.

As expected, the application of steady blowing delayed the onset of vortex breakdown only when the natural burst location was upstream of the blowing port. At angles of attack when the natural burst location was downstream of the blowing port ( $\alpha \leq 19$  deg), the application of steady blowing advanced the breakdown location to the vicinity of the blowing port. The diameter of the vortices, as indicated by the dye stream, decreased noticeably during blowing. Only blowing coefficients up to 0.03 were tried since little further effectiveness was expected beyond this value,<sup>20</sup> and more importantly, this value may be the limit in practical applications. Once the natural burst point moved upstream of the port and closer to the apex, the burst was delayed by as much as 11% of root chord for the highest blowing coefficient at 22 deg. The net changes in vortex breakdown location because of steady blowing at  $C_\mu = 0.02$  and 0.03 were compared, and although the data for the two blowing coefficients generally followed a similar trend, the larger blowing coefficient resulted in a 0.05c further delay in breakdown. Beyond  $\alpha = 34$  deg (32 deg), steady blowing at  $C_\mu = 0.03$  (0.02) did not alter the burst location.

Since a noticeable difference between the effects of various blowing coefficients was observed, a  $C_\mu$  of 0.03 was used for all pulsed blowing runs. The reduced blowing frequency  $F$  was varied over the entire range of 4.8–72.1 (1–15 Hz). Pulsed blowing proved to delay vortex breakdown more effectively than did steady blowing. When the natural burst point was located downstream of the port during pulsed blowing, the vortex burst earlier than in the no-blowing case. Once the nat-

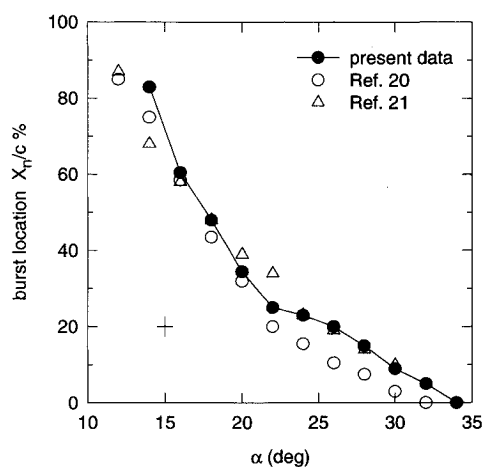


Fig. 4 Baseline (no blowing) vortex burst location; present data at  $Re = 8.6 \times 10^4$ . The experimental uncertainty is indicated by the error bars.

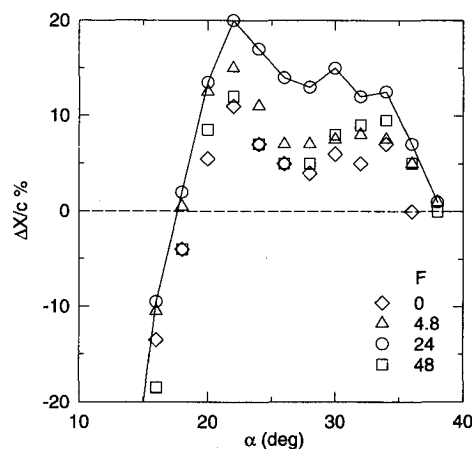


Fig. 5 Net change in the burst location for a stationary wing, steady and pulsed blowing at  $C_\mu = 0.03$  and pulsing frequencies of  $F = 48, 24$ , and 4.8.

ural burst point moved upstream of the port and closer to the wing apex, vortex breakdown was delayed by as much as 20% chord length at  $\alpha = 22$  deg and  $F = 24$  as compared to no-blowing conditions. The net change in vortex breakdown location as a function of  $\alpha$  is shown in Fig. 5 for three different reduced blowing frequencies of 4.8, 24, and 48 along with the steady blowing data. Again, all pulsed blowing data proceed in a way similar to the steady blowing data. Throughout the  $\alpha$  range, the greatest effectiveness occurred at a pulsing frequency of  $F = 24$  (5 Hz).

At this point, the natural shedding frequency of discrete vortices has to be considered. Gad-el-Hak and Blackwelder<sup>1</sup> reported that for a 60-deg delta wing the natural shedding frequency was 4.2 Hz at  $\alpha = 15$  deg and a freestream velocity of 10 cm. Normalizing this frequency by the freestream velocity and the wing root chord and varying the Reynolds number over the range of  $1.25 \times 10^4$  to  $3.33 \times 10^5$  resulted in the expression  $1625/\sqrt{Re}$  for the normalized shedding frequency at  $\alpha = 15$  deg. Moreover, the natural shedding frequency in that study varied between 3.2–2.8 Hz in the range of  $20 \leq \alpha \leq 30$  deg, and it had an average value of 2.87 Hz at a free-stream velocity of 10 cm/s. If the Reynolds number dependence at  $\alpha = 15$  deg holds for the  $\alpha$  range of interest, then for the present Reynolds number of  $8.6 \times 10^4$  the average natural shedding frequency would be 4.9 Hz  $[(2.87/4.2)(1625/\sqrt{Re})U_\infty/c]$ . The largest delay in vortex breakdown over stationary wings in the present data was observed at a pulsing frequency of 5 Hz. If one assumes that the discrete vortices in the present experiments are shed at a frequency of 4.9 Hz (equal to that inferred from the empirical relation in Ref. 1), then it can be hypothesized that RASB forcing at the natural shedding frequency of free shear layers would induce the greatest delay in vortex breakdown. Of course, this hypothesis has to be validated by further quantitative measurements.

Since the variation of the shedding frequency in the data of Ref. 1 appears to be limited to about  $\pm 11\%$  of the average value in the  $\alpha$  range of interest, one would expect that a single pulsing frequency or a narrow range of frequencies would produce the most effectiveness in terms of breakdown delay. Lowson<sup>4</sup> and Gordnier and Visbal<sup>5</sup> have reported somewhat larger (but of the same order of magnitude) shedding frequencies for 70- and 76-deg delta wings, respectively.

In the present experiments, reduced pulsing frequencies of 48 (10 Hz) and beyond resulted in negligible change above steady blowing over the  $\alpha$  range of interest. The lowest reduced frequency of 4.8 was comparable with the most effective value of  $F = 24$  up to  $\alpha = 20$  deg. Beyond this angle, the burst location for  $F = 4.8$  moved closer to the steady blowing data as  $\alpha$  increased. The angle of attack at which the breakdown reached the wing apex was increased by 4 deg in the pulsed blowing and by 2 deg in the steady blowing over the no-blowing condition. Based on the static results, all dynamic runs were conducted with blowing at  $C_\mu = 0.03$  and pulsing at  $F = 24$ , for these parameters produced the maximum delay in vortex breakdown location in static runs.

#### Dynamic Testing

Dynamic tests were designed to determine the effects of steady and pulsed blowing on the vortex breakdown location above a pitching delta wing. Values for  $\alpha^*$  were selected as 0.013, 0.040, and 0.067, which correspond to pitching rates of 1, 3, and 5 deg/s, respectively. All dynamic tests involved the first cycle of ramp-pitching motion from  $\alpha = 18$  to 32 deg and back again to 18 deg. This range was chosen because the RASB blowing scheme was ineffective outside it during static runs. At first, a series of baseline runs was conducted to assess the experimental techniques and to compare the vortex breakdown characteristics with previous studies. The burst location for the normalized pitching rate of 0.067 as a function of  $\alpha$  is contrasted against the static case in Fig. 6. As expected, a hysteresis or dynamic lag was observed for this and the other

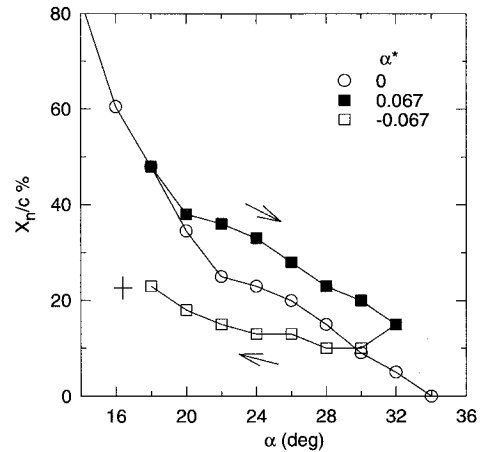


Fig. 6 Vortex burst location during ramp-pitching, no blowing. Filled symbols indicate ramp pitchup and open symbols ramp pitchdown portions of the cycle.

pitching rates as well. During pitchup, vortex breakdown was delayed by as much as  $0.11c$  at  $\alpha = 22$  and  $30$  deg; during pitchdown, vortex reformation was delayed by  $0.25c$  at the end of the cycle. The present data agree only qualitatively with the data in Ref. 17 since the magnitude of the lag in that study is about twice that in the present data for the comparable ramp pitchup rates. However, the vortex burst location propagates upstream linearly with  $\alpha$ , indicating a constant speed for the motion of burst location. This is consistent with previous studies of 60-,<sup>17,19</sup> 70-,<sup>15</sup> and 75-deg<sup>16</sup> delta wings. The discrepancy in the lag magnitude is believed to be because of the difference between the starting pitchup angle in the present study (18 deg) and Ref. 17 (12.5 deg). The wing thickness and Reynolds number in Ref. 17 were also about an order of magnitude smaller than the present values.

Once the pitching technique was validated, a complete matrix of data for the three pitching rates under no-blowing, steady, and pulsed blowing was obtained. These data are presented in two series. In the first, blowing parameters were fixed and pitching rates were varied, and in the second, blowing parameters were varied for each constant pitching rate.

The first series of data compared the vortex burst location for the three normalized pitching rates of 0.013, 0.04, and 0.067 under no-blowing, steady, and pulsed blowing conditions. The data are plotted in Fig. 7, and for clarity, the lowest pitching rate data are not included. Figure 7a revealed that as the pitching rate increased in absence of blowing, the magnitude of the hysteresis increased. The higher pitching rate also kept the burst point from reaching the apex, whereas the burst location in static conditions is near the apex at the peak  $\alpha$  of 32 deg. This effect was consistently observed through all dynamic runs. The dynamic lag resulted in a  $0.10c$  difference in vortex breakdown location between  $\alpha^* = 0.040$ – $0.067$  at  $\alpha = 32$  deg, the peak of the ramp-pitching motion. As mentioned earlier, the ramp pitchup burst locations vary linearly with  $\alpha$ , implying a constant propagation speed for the burst location. Interestingly, the ramp pitchdown data do not follow a linear variation with  $\alpha$ .

The data for steady blowing are shown in Fig. 7b. It appears that although steady blowing altered the vortex breakdown location for both pitching rates, steady blowing was much more effective in the case of slower pitching rate. The latter burst location data have become comparable to that of the faster pitching rate. In fact, the burst location for the two pitching rates coincided at the peak of pitching motion. The largest delays in the burst location were 0.10 and  $0.05c$  at  $\alpha = 32$  and  $26$  deg for the 0.04 and 0.067 ramp pitchup rates, respectively. The net delay in the breakdown location is plotted in Fig. 8 and will be further discussed subsequently. During the pitch-

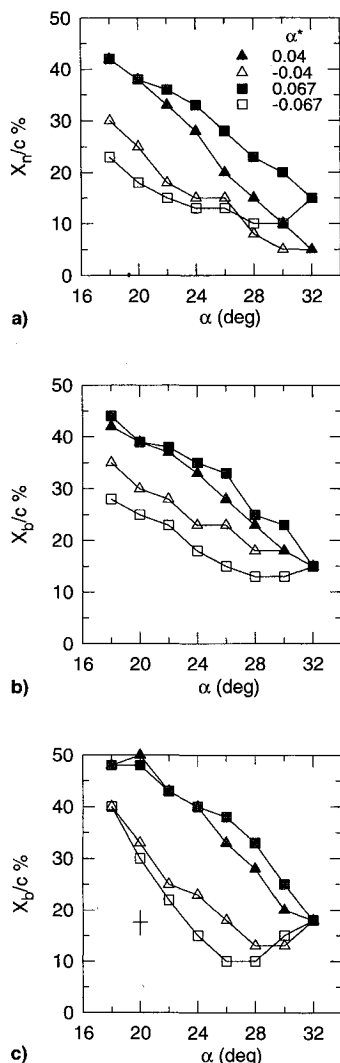


Fig. 7 Vortex burst location for 0.04 and 0.067 pitching rates: a) no blowing, b) steady blowing at  $C_\mu = 0.03$ , and c) pulsed blowing at  $C_\mu = 0.013$  and  $F = 24$ . Filled and open symbols indicate ramp pitchup and down portions of the cycle.

down portion of the cycle, steady blowing was also more effective in reforming the vortex for  $\alpha^* = 0.040$  as compared with  $\alpha^* = 0.067$ . The burst location delays were generally about 0.10 and 0.05c for  $\alpha^* = 0.040$  and 0.067 over the latter segments of the pitchdown cycle.

Pulsatile blowing data of Fig. 7c showed that even in ramp-pitching, just as in the static runs, pulsing delayed the burst location beyond that in steady blowing. Pulsed blowing was also more effective for the lower pitching rate when compared with the higher pitching rate. It can be seen in Fig. 7c that pulsed blowing resulted in a burst location difference of 0.05c or less between the two pitching rates during the pitchup part of the cycle. A notable observation in this data set is the substantial decrease in the burst location difference between the beginning and the end of the cycle as pulsatile blowing is applied. The burst locations were identical for the two pitching rates near the peak of pitchup and the final pitchdown region of  $\alpha \leq 22$  deg.

The data in the second series are depicted in Fig. 8, for which the pitching rates were held constant while blowing parameters were varied. In these plots, the ordinate reflects the increase of  $\alpha$  from 18 to 32 deg (i.e., ramp pitchup) on the left side, and the decrease of  $\alpha$  from 32 to 18 deg (i.e., ramp pitchdown) on the right side. The abscissa is the net change because of steady and pulsed blowing over the no-blowing

dynamic case. For all three pitching rates, pulsatile blowing induced greater changes during pitchup in contrast to steady blowing by about 0.05c throughout the  $\alpha$  range. At the beginning of the cycle, the delay can be as much as 0.10c for the two higher pitching rates. Moreover, the curves for steady and pulsed blowing follow similar trends for the three pitching rates during pitchup. The overall magnitude of net change offered by both steady and pulsed blowing decreases as the pitching rate is increased and is notably smaller than that observed in static conditions at  $\alpha^* = 0.067$ .

During pitchdown, steady blowing delayed the burst location further than pulsed blowing at higher angles (the first part of cycle) while pulsing was more effective at the lower angles of attack. Figure 8a demonstrates the fairly consistent delays offered by pulsed blowing over steady blowing in the range of  $28 > \alpha > 18$  deg for the normalized pitching rate of 0.013. Figure 8b shows that for  $30 > \alpha > 22$  deg steady blowing is better suited for delaying the burst location at the 0.040 pitching rate. Figure 8c provides a similar trend for  $\alpha^* = 0.067$ , with the distinction that the breakdown location moved downstream rapidly at the end of the pitchdown cycle. In general, the net changes in the burst location are comparable between pitchdown and pitchup. The delays in the burst location during dynamic runs are smaller than the ones induced by blowing on stationary wings by a factor of 2.

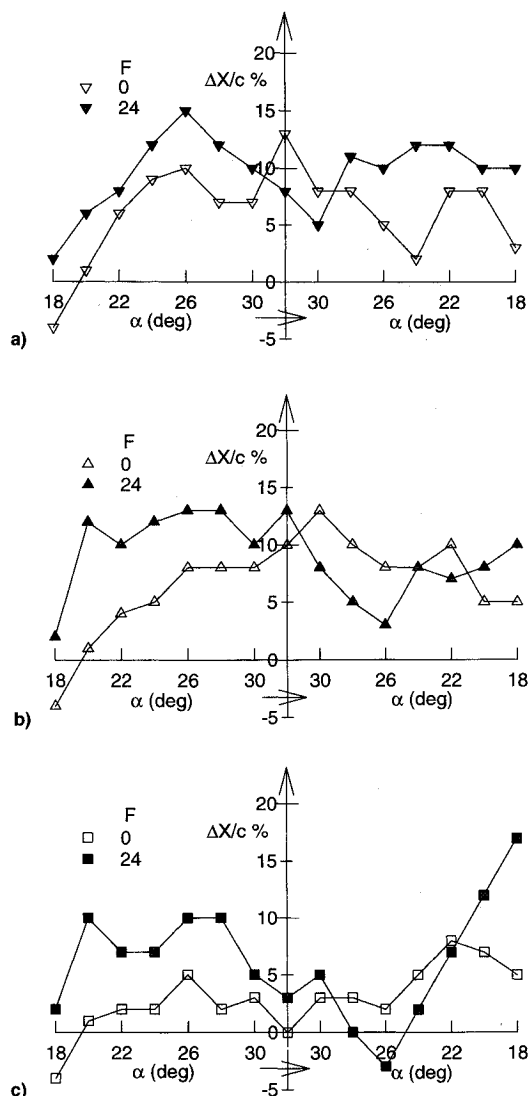


Fig. 8 Net change in the burst location because of pulsed (filled symbols) and steady (open symbols) blowing at  $C_\mu = 0.03$ :  $\alpha^* =$  a) 0.013, b) 0.04, and c) 0.067.

## Discussion

To compare the effects of blowing under static and dynamic conditions, the static (baseline) burst locations were subtracted from the static and dynamic blowing data. The resulting  $\Delta X/c$  is plotted in Fig. 9 for the largest pitching rate of 0.067. For clarity, the other pitching rate data are not included in the plot. Figure 9a compares the net changes (over the baseline) because of pitching without blowing, steady blowing in static conditions, and steady blowing while ramp-pitching. During the pitchup portion of the cycle, steady blowing during ramp-pitching provided the largest delays, as much as 0.14c at 30 deg, followed by pure pitching (no blowing) and steady blowing on the stationary wing. Both pure pitching and blowing on the stationary wing altered the burst location; however, the delays gained from steady blowing while pitching were not equal to the sum of the two. In fact, at this pitching rate, steady blowing while ramp-pitching followed and produced results quite close to that of pitching alone. This was true for ramp pitchup as well as ramp pitchdown portions of the cycle.

Effectiveness of pulsed blowing during ramp-pitching is contrasted against the data from pure pitching and pulsed blowing on the stationary wing in Fig. 9b. In this case, pulsed blowing altered the burst location by nearly the same amount on the stationary and pitching up wings. The data for pure pitching fall below the other two cases during the pitchup portion of cycle. Again, the sum of changes from pure pitching and pulsed blowing on the stationary wing does not equal the delays in the combined case. Pulsed blowing promoted the vortex reformation significantly only when  $\alpha < 24$  deg during the pitchdown portion of the cycle. Moreover, blowing, steady or pulsed, moved the burst location very close to its static position at  $\alpha = 22$  deg during pitchdown. Blowing was most effective at this angle of attack even in the static case.

The conclusion that emerges from the plots in Fig. 9 is that if blowing, steady or pulsed, produces changes in the burst location that are greater than that generated by pitching up alone, then blowing will alter the burst location by the same amount in static and ramp pitchup cases. In other words, when the effect of ramp-pitching is relatively small in comparison with blowing, the burst location responds in a quasisteady manner and is determined primarily by  $\alpha$  and blowing parameters. This was the case for pulsed blowing at all three pitching rates. Conversely, when the effects of pitchup surpass the delays created by blowing, the burst location will be influenced more by the pitching parameters as opposed to blowing. This was the case when steady blowing was employed at the highest pitching rate. In none of the present experiments were the delays from blowing alone and pure pitchup additive.

During the pitchdown portion of the cycle, the burst location in presence of blowing exhibited a trend that was mostly similar to the natural (no blowing) dynamic data. Blowing delayed the burst location generally between 0.05–0.10c; pulsed and steady blowing were effective to the same extent. The only exception was the case of pulsed blowing applied to the highest pitching rate, where significant changes in the vortex reformation were observed near the end of the cycle. During pitchdown, blowing and pitching have opposing influences on the burst location and it appears that the net delays due to blowing erode continually as the pitching rate is increased. The dominant factor is the pitching rate, and the present blowing scheme (RASB) has a modest effect in altering the breakdown location. Moreover, the delays caused by blowing on the stationary wing cannot be used to predict the burst location when the wing is pitching down.

The following question arises: what if the pitching rates are increased beyond the values in the present experiments with the same blowing scheme? From previous findings,<sup>15,17,19</sup> one would expect to observe a larger delay in vortex breakdown location when blowing is absent. Both ramp pitchup and blowing result in delay of vortex breakdown despite their dif-

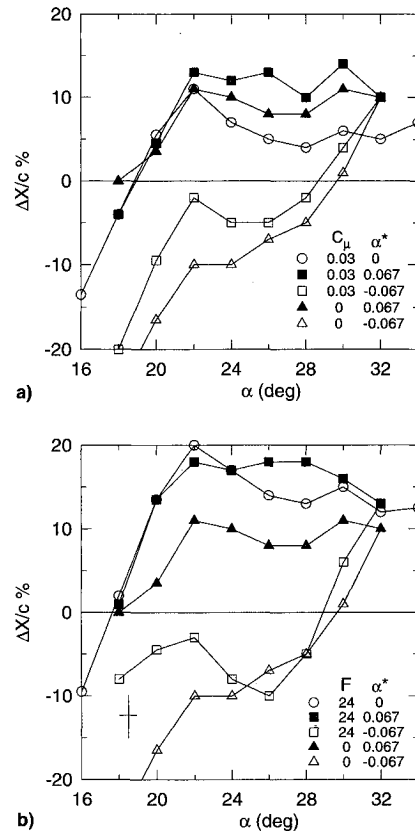


Fig. 9 Changes in the burst locations above the baseline because of ramp-pitching ( $\Delta$ ,  $\nabla$ ) at  $\alpha^* = 0.067$ , blowing on a stationary wing ( $\circ$ ), and blowing on a ramp-pitching wing ( $\blacksquare$ ,  $\square$ ): a) steady blowing at  $C_\mu = 0.03$  and b) pulsed blowing at  $C_\mu = 0.03$  and  $F = 24$ .

ferent effects on vortex stability. The present data suggest that the application of blowing will probably still delay breakdown albeit at a reduced level. At very large normalized pitching rates, the effects of blowing are expected to be overshadowed by the pitching. However, the application of blowing can nevertheless be quite useful for vortex reformation during the pitchdown cycle. At this point, a comparison of the present findings with that of Miller and Gile<sup>19</sup> is warranted since both studies considered the effects of blowing under dynamic conditions. That study utilized steady blowing along the vortex core from a tube placed externally above 60- and 76-deg sweep delta wings. Although their blowing coefficients and normalized pitching rates were larger than those used in the present experiments, similar results were obtained. Namely, blowing altered the burst location in both pitchup and pitchdown conditions. For the one pitching rate that data were presented for the 60-deg wing, the delays from pure pitchup and blowing alone appeared to be cumulative. Upon further inspection of their plots, it turned out that at this specific pitching rate, the blowing and pitching alone generated very comparable delays on the vortex burst location, and neither one was dominant. This seems to be an instance between the two limits of quasisteady and pitch-dominated behavior discussed earlier.

Another issue that needs to be addressed involves the optimum blowing parameters when the wing is experiencing ramp pitching motions. In the present study, only blowing conditions that created the largest breakdown delays in the static case were applied in the dynamic tests. It is possible to investigate whether larger blowing intensities can significantly alter the burst location in the ramp pitching runs. However, appreciably larger blowing intensities may not be feasible from a practical point of view. Moreover, previous studies<sup>20,22</sup> of the RASB method have shown that doubling the blowing coefficient for a stationary wing will not alter the burst location substantially.

If one assumes that the pulsing frequency that induced the largest breakdown delay ( $F = 24$ ) is related to the natural shedding frequency of discrete vortices in static cases, as hypothesized earlier, then the optimum pulsing frequency in dynamic conditions may also be a function of the natural shedding frequency of discrete vortices. The shedding frequency, in turn, has been observed to depend on both the freestream velocity and the angle of attack.<sup>1</sup> For a 60-deg delta wing, the reported shedding frequency in Ref. 1 varies only by about 11% over the range of interest in the present experiments. Therefore, unless the shedding frequency is strongly dependent on the pitching rate, there should be a narrow optimal pulsing frequency range for both static and dynamic cases.

### Conclusions

Pulsed blowing is an effective means of delaying vortex breakdown when the blowing port is downstream of the natural burst point in the RASB configuration. Pulsing, at the (inferred) natural shedding frequency of the discrete vortices, was capable of enhancing the vortical flow over the delta wing, and therefore, delaying breakdown. In fact, pulsatile blowing reduced the mean flow rate by one-half while delaying the burst location by significant amounts over steady blowing. The existence of a hysteresis effect during ramp-pitching, the magnitude of which increased with increasing pitching rate, was verified. Pitching upward delayed vortex breakdown while pitching downward delayed vortex reformation. Pulsed blowing consistently delayed breakdown during ramp-pitching, and it did so to a greater extent than steady blowing in nearly all cases. When the changes in the burst location because of pitching alone are relatively small in comparison with blowing, the vortex burst behaves quasisteadily, i.e., the same delays are gained under static and dynamic conditions. On the other hand, at high pitching rates, the burst location is influenced more by the pitching parameters rather than blowing. Furthermore, vortex reformation during the downstroke is facilitated by steady and pulsed blowing to about the same extent. The changes in the burst location brought about by pulsed (RASB) blowing warrant further testing on other sweep-angle delta wings, such as 70 deg. A wider range of pitching rates, perhaps on fighter models, should be investigated to confirm the present findings concerning blowing during pitching conditions. Future experiments should also address the question of dependence of optimum pulsing frequency on the pitching rate.

### Acknowledgments

The second author was supported by NASA Grant NAGW-4290. The help of undergraduate students Matthew Meyer, Michael Rhein, and Barry Rodrigues with the design and assembly of the experimental apparatus is gratefully acknowledged. The authors also wish to thank Todd Billings for his tutelage in manufacturing many of the components of the pitching mechanism.

### References

<sup>1</sup>Gad-el-Hak, M., and Blackwelder, R., "The Discrete Vortices from a Delta Wing," *AIAA Journal*, Vol. 23, No. 6, 1985, pp. 961, 962.

<sup>2</sup>Brown, G. L., and Roshko, A., "On Density Effects and Large Structure in Turbulent Mixing Layers," *Journal of Fluid Mechanics*, Vol. 64, Pt. 4, 1974, pp. 775–816.

<sup>3</sup>Winant, C. D., and Browand, F. K., "Vortex Pairing: The Mechanism of Turbulent Mixing Layer Growth at Moderate Reynolds Number," *Journal of Fluid Mechanics*, Vol. 63, Pt. 2, 1974, pp. 237–255.

<sup>4</sup>Lowson, M. V., "The Three Dimensional Vortex Sheet Structure on Delta Wings," *Fluid Dynamics of Three-Dimensional Turbulent Shear Flows and Transition*, CP-438, AGARD, Oct. 1988, pp. 11.1–11.16.

<sup>5</sup>Gordnier, R. E., and Visbal, M. R., "Unsteady Vortex Structure over a Delta Wing," *Journal of Aircraft*, Vol. 31, No. 1, 1994, pp. 243–248.

<sup>6</sup>Ho, C.-M., and Huerre, P., "Perturbed Free Shear Layers," *Annual Review of Fluid Mechanics*, Vol. 16, 1984, pp. 365–424.

<sup>7</sup>Gad-el-Hak, M., and Blackwelder, R., "Control of the Discrete Vortices from a Delta Wing," *AIAA Journal*, Vol. 25, No. 8, 1987, pp. 1042–1049.

<sup>8</sup>Shi, Z., Wu, J. M., and Vakili, A. D., "An Investigation of Leading-Edge Vortices on Delta Wings with Jet Blowing," *AIAA Paper 87-0330*, Jan. 1987.

<sup>9</sup>Gu, W., Robinson, O., and Rockwell, D., "Control of Vortices on a Delta Wing by Leading-Edge Injection," *AIAA Journal*, Vol. 31, No. 7, 1993, pp. 1177–1186.

<sup>10</sup>Vakili, A. D., Eramo, R., and Tennent, S. B., "Increasing and Decreasing the Stability of a Confined Vortex by Forcing," *AIAA Paper 93-3039*, July 1993.

<sup>11</sup>Meyer, J., and Seginer, A., "Effects of Periodic Spanwise Blowing on Delta Wing Configuration Characteristics," *AIAA Journal*, Vol. 32, No. 4, 1994, pp. 708–715.

<sup>12</sup>Gad-el-Hak, M., and Ho, C.-M., "The Pitching Delta Wing," *AIAA Journal*, Vol. 23, No. 11, 1985, pp. 1660–1665.

<sup>13</sup>LeMay, S. P., Batill, S. M., and Nelson, R. C., "Vortex Dynamics on a Pitching Delta Wing," *Journal of Aircraft*, Vol. 27, No. 2, 1990, pp. 131–138.

<sup>14</sup>Guglieri, G., Onorato, M., and Quagliotti, F., "Breakdown Analysis on Delta Wing Vortices," *Zeitschrift Flugwissenschaften Weltraumforsch.*, Vol. 16, No. 4, 1992, pp. 226–230.

<sup>15</sup>Thompson, S. A., Batill, S. M., and Nelson, R. C., "The Separated Flowfield on a Slender Delta Wing Undergoing Transient Pitching Motions," *Journal of Aircraft*, Vol. 28, No. 8, 1991, pp. 489–495.

<sup>16</sup>Magness, C., Robinson, O., and Rockwell, D., "Control of Leading-Edge Vortices on a Delta Wing," *AIAA Paper 89-0999*, March 1989.

<sup>17</sup>Miau, J. J., Chang, R. C., Chou, J. H., and Lin, C. K., "Nonuniform Motion of Leading-Edge Vortex Breakdown on Ramp Pitching Delta Wings," *AIAA Journal*, Vol. 30, No. 7, 1992, pp. 1691–1702.

<sup>18</sup>Rediniotis, O. K., Klute, S. M., Hoang, N. T., and Telionis, D. P., "Pitching-Up Motions of Delta Wings," *AIAA Paper 92-0278*, Jan. 1992.

<sup>19</sup>Miller, L. S., and Gile, B. E., "The Effects of Blowing on Delta Wing Vortices During Dynamic Pitching at High Angles of Attack," *AIAA Paper 92-0407*, Jan. 1992.

<sup>20</sup>Fitzpatrick, K., Johari, H., and Olinger, D., "A Visual Study of Recessed Angled Spanwise Blowing Method on a Delta Wing," *AIAA Paper 93-3246*, July 1993.

<sup>21</sup>O'Neil, P. J., Roos, F. W., Kegelmann, R. M., Barnett, R. M., and Hawk, J. D., "Investigation of Flow Characteristics of a Developed Vortex," *Naval Air Development Center Rept. 89114-60*, Warminster, PA, May 1989.

<sup>22</sup>Johari, H., Olinger, D. J., and Fitzpatrick, K. C., "Delta Wing Vortex Control via Recessed Angled Spanwise Blowing," *Journal of Aircraft*, Vol. 32, No. 4, 1995, pp. 804–810.